View metadata, citation and similar papers at core.ac.uk
brought to you by CORE
provided by SINERGI

SINERGI Vol. 24, No. 2, June 2020: 117-124
http://publikasi.mercubuana.ac.id/index.php/sinergi
http://doi.org/10.22441/sinergi.2020.2.005

THE INVESTIGATION OF END MILL FEEDS ON CNC ROUTER MACHINE USING VIBRATION METHOD

Agung Wahyudi Biantoro*, Heru Maryanto, Arif Kusnan Hidayanto, Abdul Hamid
Mechanical Engineering Vibration Laboratory, Universitas Mercu Buana,
Jalan Meruya Selatan No. 1, Kembangan, Jakarta Barat 11650, Indonesia
*Corresponding Author Email : agung_wahyudi@mercubuana.ac.id

Abstract -- *Vibration on End Mill Feeds will occur due to friction between the workpiece and end mill. The friction which occurs will cause tool wear in the insert blade. At this point, the tool wear experienced by the end mill can be seen from the imperfect feed of the workpiece that is resulted. Therefore, it is necessary to find out a method that can quickly and accurately detect tool wear at the end mill. The one that was experimented in this study was the vibration method. The vibration response was measured at their x, y, and z axes with rotation speeds of 2500 rpm, 3500 rpm, and 4500 rpm. At the broken end mill, it was shown that frequencies resulted did not affect the rotation while in the standard end mill. The initial frequency was highly influenced by spindle rotations treated on it.*

Keywords: *CNC Milling; Vibration Method; Frequency Response Function; End Mill; Rotary Speed*

Copyright © 2020 Universitas Mercu Buana. All right reserved.

Received: October 21, 2019 *Revised: December 24, 2019* *Accepted: January 15, 2020*

INTRODUCTION

The use of a CNC machine can be found in various industries ranging from big to medium scale. Those industries produce components that can be remanufactured for several times with high accuracy and precision [1]. High Speed Machining, tool breakage prevention, thin wall deflection, tool geometry, and chatter monitoring are studied in relation to the five performance indicators, respectively [2].

Vibration feeding at the *end mill* frequently causes friction between the object and end mill, which leads to the occurrence of tool wear at the insert parts. The tool wear of an end mill can be detected from the imperfect feed that it results in. Therefore, a quick and accurate method is needed to find to identify the tool wear at the end mill.

One of the methods widely utilized to identify the tool wear at the end mill is the vibration method. Vibration in a workpiece and chisel is a dependent variable that refers to the vibration resulted from the feeding process during the machining process taking place. Vibration resulted from the machining process in milling is highly influential on the product quality, like sometimes it will produce rough surfaces. Wijayanto conducted a study to identify the effect of feed rate on surface hardness in CNC Router 3 axis machining on Teflon material [3]. Sutanto et al. utilized the Frequency Response Function (FRF) method to study the damage at the endmill based on the vibration response [4]. The material removal changes the natural frequency and modal shape of the system, which causes the variation of the limit on cutting depth [5].

Preliminary cutting tests show that the cutting forces are reduced by over 30% with the ultrasonic vibration assisted milling and drilling operations [6]. Studies on FRF have been widely carried out at Mercu Buana University, especially at the vibration laboratory. This method has the purpose of finding some non – linear signals [7]. In that study, he obtained a global vibration mode frequency from a cylindrical piston motor with some dynamic characteristics. Subekti using the FRF method, also said there is a natural frequency in diesel engines that appears in more than one measurement point [8]. This frequency shows the existence of a global vibration mode. A year later, those dynamic characteristics were then applied by Efendi et al. at a disc brake utilizing bump test and discovered two types of frequencies, global and local [9].

Furthermore, this research continues to study the characteristics of damage to the disc brake [10]. The frequency is smaller than the natural frequency at the FRF point. With the bearing house, there are differences in the three axes of the test results. On the X and Y axis, there are two vibrate modes, namely at the natural frequency 8 and 35 Hz [11].

CNC *milling* is a machine that is controlled by the CNC program with the movements in the X and Y axes and spindles in the Z-axis or cutter house based on the instruction from the user [12].

This machine uses a Cartesian coordinate system, as can be seen in Figure 1.

At the *end milling*, the tooth cutter of a chisel is located in sheet and at the end of a body. The axis rotates perpendicular to the surface of the workpiece and can move at an angle [12].

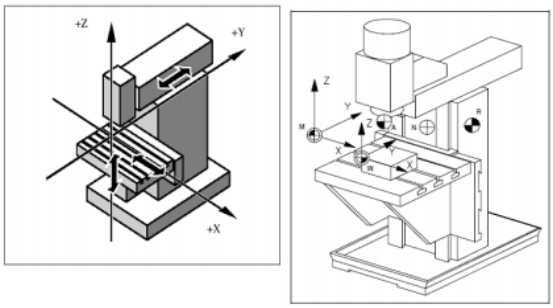

Figure 1. The coordinate system of the CNC milling machine

MATERIAL AND METHOD

The velocity of feeding is the distance of movement of the workpiece with forwarding motion stated in millimeters per second or feeds per second. Feeding velocity and chopping velocity have different purposes. Cutting speed (V_c) is used to identify the speed of machine rotation or RPM while the table feed (Vf) emphasizes the velocity of Frais table feeding when cutting the workpiece [13]. The feed velocity can also be referred to as chisel feeding, which is identified by comparing the distance of workpiece per time unit and the number of teeth in cutter [14].

The feeding velocity is stated in millimeter and calculated by considering the number of blades and the speed of each Frais (f_z) blade feeding. Feed per tooth, which is stated in mm/tooth, is the value of the milling process to calculate the feed table using the following Equation (1).

$$V_f = n \times f_z \times z_n \quad (1)$$

Annotation:
V_f = table feed (mm/minute)
n = spindle rotation speed (rpm)
f_z = feed per tooth (mm)
z_n = the number of blades

Feed per revolution stated in mm/rev is exclusively used to calculate the feed and the finishing ability of a cutter. Feed per revolution is a complimentary scale to indicate how far the chisel moves when rotating based on Equation (2).

$$f_n = \frac{Vf}{n} \quad (2)$$

Annotation:
f_n = feed per revolution (mm/rev)
V_f = table feed (mm/minutes)
n = rotation speed (rpm)

While calculating the cutting time, we used Equation (3).

$$t_c = \frac{lt}{Vf} \quad (3)$$

Annotation:
l_t = cutting length (mm)
t_c = cutting time (minutes)

Feed per tooth (f_z) is the score of the milling process to calculate the table feed. If the cutter milling has more than one blade, the value of f_z must be included in the calculation. The value of feed per tooth is calculated based on the thickness of the chips, which are recommended. The determination of the feeding rate should be calculated and adjusted with the size of the chisel and the number of blades. Following is a feeding movement table per tooth recommended for the milling process using HSS chisel [15].

The thickness of feed or cut depth is determined based on the difference between the depths of the workpiece before and after treated. It can be selected based on the material of the workpiece, knife, machine, throttling system, and cutting time [16]. The damping alloy can reduce machining vibration regardless of workpiece materials or the form of it, and the sleeve type tool holder improves the surface roughness significantly in an end-milling process for both workpiece materials [17]. In the milling process, we normally design five different depths, which are 0,2 mm; 0,4 mm; 0,6 mm; 0,8 mm and 1 mm [18]. Firmansyah et al. determine the effect of variations in the depth of burial (0.4 mm, 0.6 mm, 0.8 mm) and speed feeds on the workpiece surface roughness in aluminum 2036 CNC milling machine TU-3A with absolute program G01. The study is for knowing the effect of variations in the numbers of slice chisel cutter endmill two flutes and four flutes [19].

The present investigation suggests that when face milling a workpiece, the over a vice height of the workpiece should not exceed 1.5 times its width [20]. The influence of the geometrical parameters and cutting parameters on the cutting forces, and give various information to establish next to the optimal trajectories of the tool during plunge milling operations on titanium alloys, according to the type of workpieces [21]. The impact of the damping system used is effective in decreasing tool vibration, and the bigger the spheres used in the damper, the higher is their effects to damp the system [22].

The cutter body geometry has a significant impact on mode shapes. The cutting performance

tests show that the milling cutter with a diameter of 125 mm performs the best in terms of static force and maximum dynamic force in the Z direction and wear resistance [23]. Variation in surface roughness was within 0.20 to 0.50 µm for experimentation irrespective of the variables and tool condition [24]. Variation in amplitudes and displacements is identified as the minimized vibration levels for varying cutting conditions [25]. In this paper, we are to discuss the effect of feed rate on the breakage of blades at insert using vibration analysis.

The milling system of vibration analysis is predictive maintenance employed to supervise and analyze the critical condition of the machine by paying attention to particular components and parts based on the vibration it produces. This analysis approach has some advantages, e.g., it can identify problems in a machine before there is a severe malfunction occurring. Besides that, the analysis can identify if there is a component of the machine experiencing failure by looking at the data of time and frequency of vibration. The vibration system at the end mill can be seen in Figure 2. Postela et al. carried out the investigation on vibration and force at the end of a chisel using a low-cost accelerometer installed in stationary spindle houses with a higher speed of CNC machine [24].

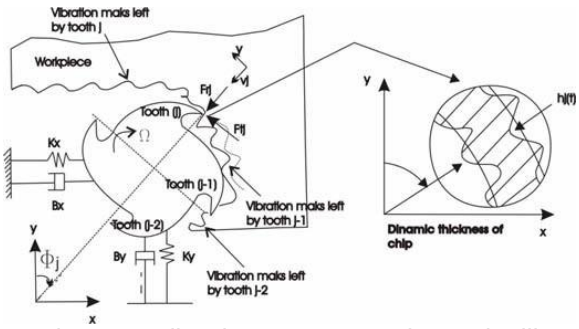

Figure 2. Vibration System at The End Mill

To measure the tool wear of the end mill, we use CNC 4 axis machine as depicted in Figure 3. The CNC 4 axis machine was produced by my students of Vibration Laboratory, Mechanical Engineering, Mercu Buana University, Jakarta with specifications as listed in Table 1.

The identification of damage that occurred at the end mill was carried out by varying the spindle rotations into 2500 rpm, 3500 rpm, and 4500 rpm. The G-code program, which was developed in the CNC 4 axis machine, had some spindle rotations, as presented in Table 2.

Table 1. Specifications of CNC machine engineer

Table Size	270 mm x 300 mm
X, Y, Z over travel	226 mm x 324 mm x 60 mm
Stepper Motor	Jk57HS56-2804, 57HS7630A4-11
Power Supply	24 V, 20 A
Spindle Motor	220 V, 500 W DC
Max. Spindle Speed	12000 rpm
Collet	ER11
Software Compatibility	Mach3
Driving System	1204 Ball Screw
Controller	BL-UsbMach-V2.0
Chuck Rotary 4 Axis	BL-UsbMach-V2.0

Figure 3. CNC 4 Axis Machine

Table 2. G-code of spindle rotation variations

Spindle rotation		
2500 rpm	**3500 rpm**	**4500 rpm**
M3 S2500	M3 S3500	M3 S4500
G0 X0 Y0 Z5	G1 Z-1 F100	G1 Z-1 F100
G1 Z-1 F100	G1 X25	G1 X25
G1 X25	G0 Z5	G0 Z20
G0 Z5	G0 X0 Y10	G0 X0 Y0
G0 X0 Y5		M5
		M30

The vibration response measurement was carried out on three axes (x, y, and z axes, respectively), as shown in Figure 4.

(a) (b) (c)

Figure 4. Vibration of measurement

In this study, the measurement of vibration was carried out with a frequency range of 1 - 1200 Hz. While a photo set up of testing to obtain experimental data can be seen in Figure 5. The vibration response read by the vibration analyzer was analyzed using MATLAB.

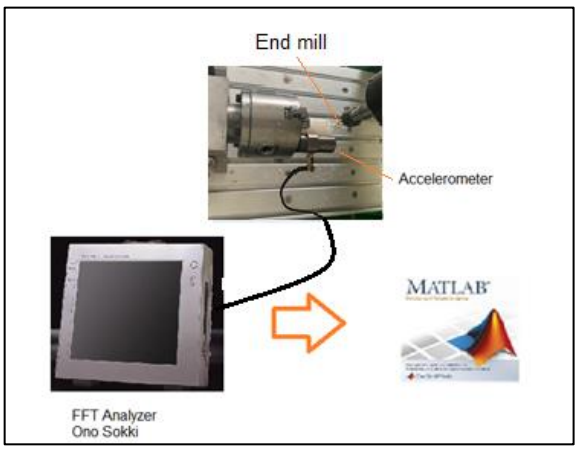

Figure 5. Photos of Setting-up the vibration testing

In Figure 5, it can be seen the equipment used that is listed as follows:

- The accelerometer sensor serves to measure response vibrations
  Type: Piezoelectric accelerometer
  Conversion sensitivity ratio: pCs^2 m 5.0- 7.0
  Frequency range, Hz: 2 -10000 Hz
  Resonance frequency:> 28 kHz
  Transverse sensitivity: <5%
  Accelerometer cable: 1.5 m
- FFT portable type analyzer CF-3600A (4-ch) with a touch panel computer was utilized for simultaneous analysis and recording. The maximum frequency that can be analyzed is 40 kHz. It was produced by Ono Japanese Sokki.
- FFT was used as a spectrum analyzer and data acquisition.
- The end mill, which was used, was Super hard end mill produced by NACHI type 4SE List6210 with the size of 3 x 9 x 50 x 6.
- Material that was used was Teflon or polytetrafluoroethylene (PTFE). The physical properties of the material can be seen in Table 3.

Table 3. Physical Characteristics of Material

No	Property	Value
1	Density	2200 kg/m^3
2	Melting point	327 ^{o}C
3	Modulus young	0.5 GPa
4	Yield strength	23 Mpa
5	Friction coefficient	0.05 – 0.10

RESULTS AND DISCUSSION

Testing was conducted by observing the feed of workpiece (Teflon) with a thickness of 1 mm and rotation speeds of 2500 rpm, 3500 rpm, and 4500 rpm.

At the first stage, the treatment was applied in X-axis with the speed of 2500 rpm by using normal and broken end mills. The graph is shown below in Figure 6.

Normal and broken Endmills were used in this study to compare frequency and amplitude rates that had been obtained. The normal end mill resulted in a frequency of 51 Hz and amplitude 6,1062 m/s^2 while the broken end mill had a frequency of 1431 Hz and amplitude 0,77681 m/s^2.

The second trial was performed at the x-axis with the rotary speed of 3500 rpm, which also used both normal and broken end mills. The results are shown in Figure 7.

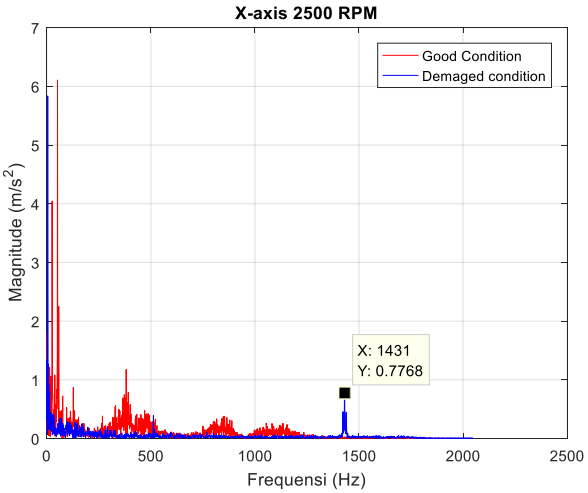

Figure 6. Graph of end mill vibration with the speed of 2500 RPM in X-axis

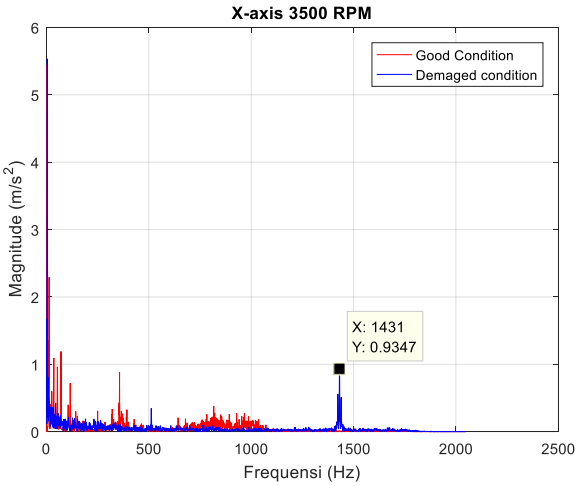

Figure 7. Graph of End Mill Vibration at the Speed of 3500 RPM in the X-axis

It can be seen in the graph that the normal end mill showed frequency 13 Hz and amplitude 2,2911 m/s^2 while the broken one showed a frequency of 1431 Hz and amplitude 0,93468 m/s^2.

Another experiment at the X-axis was performed with the rotary speed of 4500 rpm. The results are presented in Figure 8. It also tested both normal and broken end mills.

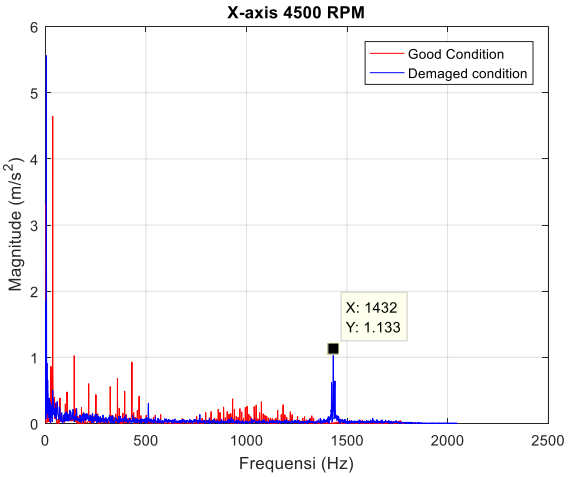

Figure 8. Graph of End Mill Vibration at the speed of 4500 RPM at X-axis

The normal end mill resulted in a frequency of 36 Hz and amplitude 4.642 m/s^2 while the normal one had a frequency of 1432 Hz and amplitude 1,1331 m/s^2.

The first experiment performed at Y-axis was at the speed of 2500 rpm using normal and broken end mills. The results are shown in Figure 9 and Figure 10.

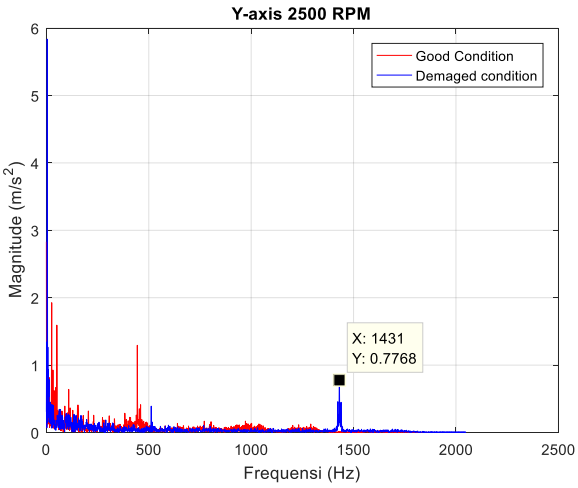

Figure 9. Graph of End Mill Vibration at the Speed of 2500 RPM at Y-axis

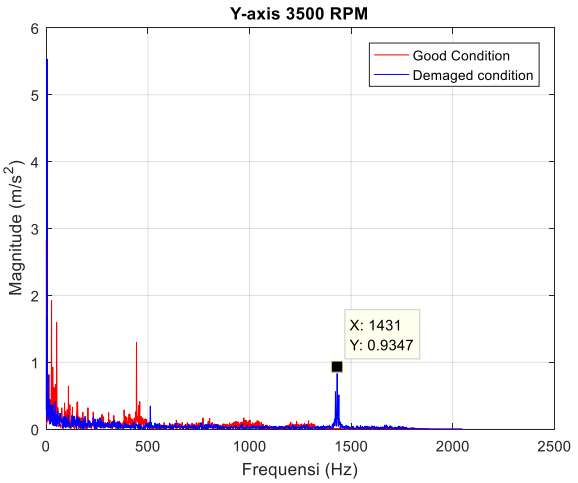

Figure 10. Graph of End Mill Vibration at the Speed of 3500 RPM at Y-axis

The normal end mill had a frequency of 26 Hz and amplitude 1.9262 m/s^2 while the broken end mill had a frequency of 1431 Hz and amplitude 0,77681 m/s^2.

Following that, another experiment was carried out at the y-axis with the rotary speed of 3500 rpm of normal and broken end mills. The frequency and amplitude can be seen in Figure 10.

The normal end mill showed a frequency of 26 Hz and amplitude 1,9262 m/s^2, whereas the broken end mill had a frequency of 1431 Hz and amplitude 0,93468 m/s^2.

The last trial at Y-axis was with the speed of rotation of 4500 rpm. It was also performed at both standard and broken end mills. The results are depicted in Figure 11.

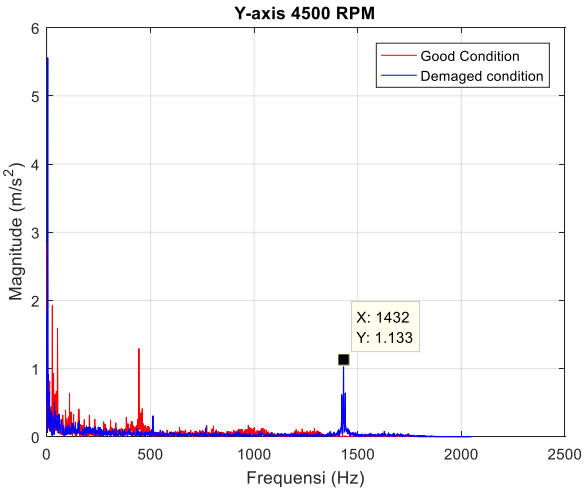

Figure 11. Graph of End Mill Vibration at the Speed of 4500 RPM at Y-axis

The normal end mill obtained a frequency of 26 Hz. Its amplitude was 1,9262 m/s^2. On the contrary, the broken one had a frequency of 1432 Hz and amplitude 1,1331 m/s^2. Similar to the previous axes, the experiment carried out at Z-axis was begin with the implementation of the rotation speed of 2500 rpm using normal and broken end mills. The data are presented in Figure 12.

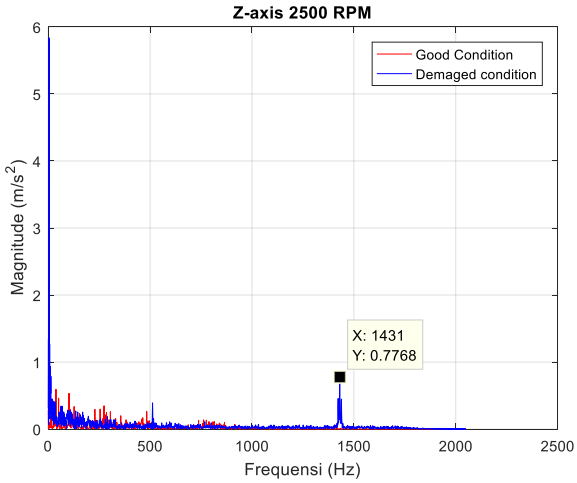

Figure 12. Graph of End Mill Vibration at the Rotation Speed 2500 RPM at Z-axis

At this rotation speed, the normal end mill showed a frequency of 38 Hz and amplitude 0.59446 m/s^2 while the broken end mill indicated the frequency of 1431 Hz and amplitude 0,77681 m/s^2. The next treated rotary speed was 3500 rpm. It also occupied normal and broken end mills, as shown in Figure 13.

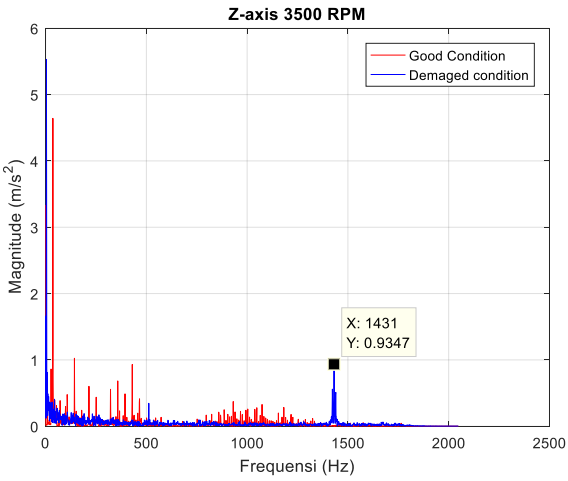

Figure 13. Graph of End Mill Vibration with the

The normal end mill had a frequency of 36 Hz and amplitude 4,642 m/s^2 while the broken one showed the frequency of 1431 Hz and amplitude 0,93468 m/s^2.

Lastly, the experiment on the Z-axis was performed at the rotary speed of 4500 rpm using both normal and broken end mils. The results are presented in Figure 14.

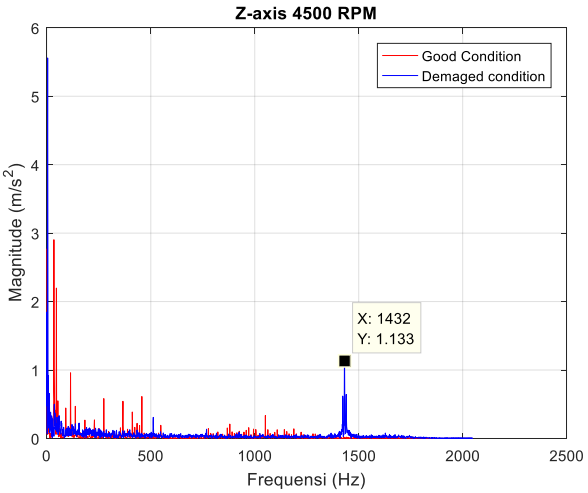

Figure 14. Graph of End Mill Vibration at a Rotary Speed of 4500 RPM at Z-axis

The frequency of the normal end mill was 34 Hz, while the broken one was 1432 Hz. The amplitudes of the normal and the broken end mills were 2,9037 m/s^2 and 1,1331 m/s^2, respectively. The data are summarized in Table 4.

The data were based on the measurement carried out at CNC 4 *axis* machine at three different axes (X, Y, and Z) with a feed value of 0.1 mm and three different rotary speeds (2500 rpm, 3500 rpm, and 4500 rpm). One of the end mill blades occupied in this study was normal while another one was broken. The workpiece used was Teflon. This material was selected considering the properties it has, including low hardness and its ability to be utilized in any conditions.

Damages on end mills generally occur as a result of frequent friction between end mill and workpiece so that the tip of blade experiences tool wear. Therefore, a regular check is necessary to carry out before using the tool.

Table 4. Data of Frequency and Amplitude at each Axis

Axis		2500 rpm		3500 rpm		4500 rpm	
		Normal	Broken	Normal	Broken	Normal	Broken
X	f (Hz)	51	1431	13	1431	36	1432
	A (m/s^2)	6.1052	0.77081	2.2911	0.93468	4.642	1.1331
Y	f (Hz)	26	1431	26	1431	26	1432
	A (m/s^2)	1.9262	0.77681	1.9262	0.93488	1.9262	1.1331
Z	f (Hz)	36	1431	36	1431	34	1432
	A (m/s^2)	0.5945	0.77681	4.642	0.93468	2.9037	1.1331

Test performed based on vibration results. Broken end mil produced significantly higher frequency compared to the normal one. It is because the broken end mill results in the unperfected feed so that the vibration is much stronger than the normal end mill.

CONCLUSION

Based on the finding and discussion presented above, there are some conclusions. The vibration method can detect damage at end mill by using a sensory put at X, Y, and Z axes at the rotary, as can be seen in the graphs. Frequency resulted from broken end mill was far higher than from the normal one due to the inability of the broken end mill to produce perfect feed causing it to experience much stronger vibration compared to the normal end mill.

REFERENCES

[1] S. Krar, and A. Gill, *Computer Numerical Control Programming Basics*, Industrial Press Inc. 200 Madison Avenue, New York, NY 10016, 1990.

[2] J. P. T. Mo, and S. Ding, "Systems Engineering for Machining," In Stjepandić J., Wognum N., J. C. Verhagen W. (eds) *Systems Engineering in Research and Industrial Practice*. Springer, Cham. 2019. DOI: 10.1007/978-3-030-33312-6_11

[3] D. Wijayanto, "Pengaruh Tool Path Dan Feed Rate Pada Proses Mesin CNC Milling Router 3 Axis Dengan Material Acrylic," *Thesis*, Universitas Muhammadiyah Surakarta, 2016, pp. 1-14.

[4] A. Susanto, C. H. Liu, K. Yamada, Y. R. Hwang, R. Tanaka, and K. Sekiya, "Milling process monitoring based on vibration analysis using Hilbert-Huang transform," *International Journal of Automation Technology,* vol. 12, no. 5, pp. 688–698, September 2018. DOI: 10.20965/ijat.2018.p0688

[5] L. Han, R. Liu, X. Liu, "Theoretical modeling and chatter prediction for the whirling process of airfoil blades with consideration of asymmetric FRF and material removal." *International Journal of Advanced Manufacturing Technology,* vol. 106, pp. 2613–2628, 2020. DOI: 10.1007/s00170-019-04799-4

[6] J. Gao and Y. Altintas, "Development of a Three-Degree-of-Freedom Ultrasonic Vibration Tool Holder for Milling and Drilling," in *IEEE/ASME Transactions on Mechatronics*, vol. 24, no. 3, pp. 1238-1247, June 2019. DOI: 10.1109/TCMECH.2019.2906904

[7] S. Subekti, A. Hammid, and A. W. Biantoro, "Identifying the Nonlinearity of Structures Dynamics by Wavelet Packet Decomposition," *Material Science and Engineering*, vol. 453, pp. 012003, June 2019. DOI: 10.1088/1757-899X/453/1/012003

[8] S. Subekti, "Studying the Dynamic Characteristics To Lengthen the Operating Life for a Diesel Engine Using Frequency Response Function (FRF) Measurement," *SINERGI*, vol. 22, no. 3, pp. 161-168, October 2018. DOI: 10.22441/sinergi.2018.3.004

[9] B. D. Efendi, S. Subekti, and A. Hamid, "Karakteristik Dinamik Disc Brake Daihatsu Sigra 1200 cc dengan Metode Bump Test," *Flywheel: Jurnal Teknik Mesin Untirta*, vol. 5, no. 1, pp14-19, April 2019.

[10] S. Subekti, et al. "Inspecting a Bump Test in the Maintenance of a 1200-cc Daihatsu Sigra Disc Brake," *SINERGI,* vol. 23, no. 3, pp. 191-198, October 2019. DOI: 10.22441/sinergi.2019.3.003.

[11] A. Susanto, S. Q. Yusuf, A. Hamid, H. Wahyudi, S. Subekti, "Implementation of Frequency Response Function on Tapper Bearing Maintenance," *SINERGI,* vol. 23, no. 2, pp. 132-138, June 2019. DOI: 10.22441/sinergi.2019.2.006

[12] A. B. H. Bejaxhin, and G. Paulraj, "Experimental investigation of vibration intensities of CNC machining centre by microphone signals with the effect of

TiN/epoxy coated tool holder," *Journal of Mechanical Science and Technology*, vol. 33, pp. 1321–1331, 2019. DOI: 10.1007/s12206-018-1232-3

[13] M. K. Dikshit, A. B. Puri and A. Maity, "Analysis of rotational speed variations on cutting force coefficients in high-speed ball end milling," *Journal of the Brazilian Society of Mechanical Sciences and Engineering,* vol. 39, pp. 3529-3539, 2017. DOI: 10.1007/ s40430-016-0673-9

[14] G. Kiswanto, M. Azmi, A. Mandala, and T. J. Ko, "The Effect of Machining Parameters to the Surface Roughness in Low Speed Machining Micro-milling Inconel 718," in *IOP Conference Series: Materials Science and Engineering,* vol. 654, 012014, 2019. DOI: 10.1088/1757-899X/654/1/012014

[15] K. Mughal, M. Q. Saleem, and M. P. Mughal, "Performance evaluation of nano-composite ceramic-coated high-speed steel (HSS) drills in high-speed machining," *International Journal of Advanced Manufacturing Technology,* vol. 96, pp. 4195-4203, 2018. DOI: 10.1007/s00170-018-1829-9

[16] F. Wang, X. Cheng, Y. Liu, X. Yang, and F. Meng, "Micromilling simulation for the hard-to-cut material," *Procedia Engineering,* vol. 174, 693-699, 2017. DOI: 10.1016/j.proeng. 2017.01.209

[17] M. Kim, J. Kim, M. Lee, and S. Lee, "Surface finish improvement using a damping-alloy sleeve-insert tool holder in the end milling process," *International Journal of Advanced Manufacturing and Technology,* vol. 106, pp. 2433–2449, 2020. DOI: 10.1007/s00170-019-04757-0

[18] H. Abbas, Pengaruh parameter Pemotongan Pada Operasi Pemotongan Milling Terhadap Getaran dan Tingkat Kekasaran Permukaan (Surface Roughness)," *Proceeding SNTTM XII & Lomba Rancang Bangun Mesin,* Lampung, Indonesia, 2013.

[19] Y. R. Firmansyah, and B. A. Hasyim, "Pengaruh Jumlah Mata Sayat Endmill Cutter, Kedalaman Pemakanan Dan Kecepatan Pemakanan (Feeding) Terhadap Tingkat Kekasaran Permukaan Benda Kerja Pada Mesin Miling CNC Tu-3a Dengan Program G01," *Jurnal Teknik Mesin*, vol. 03, no. 02, pp. 38-43, 2014.

[20] A. Bouchareb, A. Lagred, and A. Amirat, "Effect of the interaction between depth of cut and height-to-width ratio of a workpiece on vibration amplitude during face milling of C45 steel," *International Journal of Advanced Manufacturing and Technology*, vol. 104, pp.1221–1227, 2019. DOI: 10.1007/s00170-019-03944-3

[21] M. Fredj, F. Monies, W. Rubio, and J. Senatore, "Influential Parameters in Plunge Milling for Titanium Alloy Ti-6Al-4V." In: Cavas-Martínez F., Eynard B., Fernández Cañavate F., Fernández-Pacheco D., Morer P., Nigrelli V. (eds) *Advances on Mechanics, Design Engineering and Manufacturing II*. Lecture Notes in Mechanical Engineering. Springer, Cham, 2019. DOI: 10.1007/978-3-030-12346-8_37

[22] F. A. M. Galarza, M. V. de Albuquerque, A. Í. S. Antonialli, "Design and experimental evaluation of an impact damper to be used in a slender end mill tool in the machining of hardened steel," *International Journal of Advanced Manufacturing and Technology,* vol. 106, pp. 2553–2567, 2020. DOI: 10.1007/s00170-019-04786-9

[23] Li, N., Chen, Y. & Kong, D. Effect of cutter body geometry in Ti-6Al-4V face-milling process, *International Journal of Advanced Manufacturing and Technology,* vol. 100, pp. 1881–1892, 2019. DOI: 10.1007/s00170-018-2794-z

[24] S. Ehsan, S. A. Khan, M. P. Mughal, "Milling of Ti-6Al-4V alloy using hybrid geometry tooling," *International Journal of Advanced Manufacturing and Technology,* vol. 105, pp. 5045–5059, 2019. DOI: 10.1007/s00170-019-04613-1

[25] M. Postel, D. Aslan, K. Wegener, and Y. Altintas, "Monitoring of vibrations and cutting forces with spindle mounted vibration sensors," *CIRP Annals*, vol. 68, no. 1, pp. 413-416, 2019. DOI: 10.1016/j.cirp.2019. 03.019